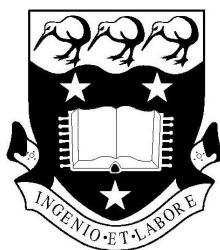


Photon correlations in Two mode cavity QED in an external magnetic field.

Esteban Canseco Viveros

Supervisor: Professor Howard J. Carmichael

The University of Auckland 2008



Abstract

We compute photon correlation functions in a cavity QED system where a single atom couples to two cavity modes with orthogonal linear polarisations, in the presence of a weak external magnetic field. We take into account the full atomic level structure for an $F=3$ to $F'=4$ transition (specifically a transition in Rubidium 85), and consider the case where one cavity mode is resonantly driven by a coherent field, while light in the other cavity mode is generated only through atomic emission. In order to study this system, we extended a previous model for the case of no field developed by M. Kronenwett, in order to include the Zeeman effect due to the magnetic field.

We use standard quantum regression formulas and numerical solutions of the master equation for the system density operator to compute steady-state properties and photon correlation functions in the weak-excitation regime. From a Monte-Carlo simulation based on a quantum trajectory we explore higher levels of excitation.

Contents

1	Introduction	3
2	Background	5
2.1	Experimental Setup	5
2.2	Interactions in a driven atom-cavity system	5
2.3	Selection Rules	8
2.4	Hamiltonian of a driven single-atom two-mode cavity system	9
3	Hamiltonian of a driven single-atom two-mode cavity system in the presence of a magnetic field	12
3.1	Hyperfine structure in an external magnetic field	12
3.2	Hamiltonian	14
4	Open Quantum Systems	18
4.1	The Master Equation approach	18
4.2	Quantum Trajectory approach	21
5	Numerical simulations: 2-mode cavity QED	24
5.1	Master Equation	24
5.2	Quantum Trajectory	30
6	Conclusion	33
6.1	Summary	33
6.2	Future Work	33
	References	34

1 Introduction

Einstein's description of the photoelectric effect and the ultraviolet photoionization of gases constitutes the first application of quantum electrodynamics and the first description of quantized electromagnetic phenomena. Einstein wrote

The wave theory of light which operates with continuous functions in space has been excellently justified for the representation of a purely optical phenomena and it is unlikely ever to be replaced by another theory. One should, however, bear in mind that optical observations refer to time averages and not to instantaneous values and notwithstanding the complete experimental verification of the theory of diffraction, reflection, refraction, dispersion and so on, it is quite conceivable that a theory of light involving the use of continuous functions in space will lead to contradictions of experience, if it is applied to the phenomena of the creation and conversion of light

Since Purcell first pointed out that a resonator could alter the atomic spontaneous emission rate. Cavity QED experienced an interest and a growing field.

In the 1950s, R. H. Brown and R. Q. Twiss investigated temporal correlations of the intensity fluctuations in a light beam emitted by a thermal source. They found out that light beam tended to arrive in bunches, rather than strictly at random. Their observation can also be explained classically as a pure wave effect of the electromagnetic light field.

There is another phenomenon, photons can also tend to arrive more evenly spread out than strictly at random. This is called photon antibunching, this effect is only understood through a quantum mechanical description; it has no classical analog or explanation.

The Jaynes-Cummings model describes a single two level atom interacting with a single mode of the radiation field. This model represents the interaction between light and matter. Despite its simplicity it contains a lot of information of the systems, such as collapse and revival.

Not only is cavity QED of interest to have a better understanding of quantum phenomena, but for its applications. Cavity QED is being a subject of study for several years, due to the fact that it is promising application in the area of Quantum Information Processing. Application of Cavity QED systems derives mostly from the ability to coherently intra-convert quantum states between material qubits (such as trapped atoms or semiconductors dot system) and photon qubits.

The principal objective of this work is the inclusion of the effects of a weak external magnetic field, to a previous theoretical model for a two-mode single atom cavity QED (especially for a Rubidium-85 atom). Investigate the second order photon correlations

and how the introduction of detunings affect this correlations. In the first chapter we will cover the experimental setup, and how this sytem is model. In the second chapter we present the Zeeman effect in the hyperfine structure for weak fields. Posterior we present the numerical approaches namely the master equation and the quantum trajectories method. Finally we present the data obtained from this numerical simulations and compared it qualitatively with the experimental data.

2 Background

The starting point for our project is the thesis done by Matthias Kronenwet, he developed a model in order to predict data for the measurments performed by L. A. Orozco's group at the University of Maryland. In the first chapter we will present the experimental set-up of Orozcos's experiment and give an overview. As well we will present and explain the theoretical model for that particular system.

2.1 Experimental Setup

The cavity QED system we are considering consists of a single ^{85}Rb resting in the center of a high-finesse optical resonator. Actually the atom is not in the center of the cavity, rather it transverse the cavity. A schematic of the experimental apparatus is shown in figure 1 Two optical cavity modes with orthogonal linear polarization on resonance with the atom via the D_2 -line $F = 3$ to $F' = 4$ transition. A weak external magnetic field induces a quantisation axis such that one mode couples the $F = 3$ atomic ground state to the $F' = 4$ excited state via $\Delta m_F = 0$ transitions. This mode is driven on-axis by a coherent field of amplitude \mathcal{E} . The other mode, with orthogonal polarisation to the driven mode, couples the atomic levels via $\Delta m_F = \pm 1$ transitions. Thus, any light in this non-driven mode originates only from a spontaneous emission event of the atom with $\Delta m_F = \pm 1$.

The light leaking out through the cavity mirror is split by a polarising beam splitter (PBS), such that the output from each mode can be detected separately. To determine and characterise properties of such systems one typically measures photon arrival times at the detectors.

In the two-mode cavity QED system being considered our main interests are the photon self and cross-correlations for the two modes.

2.2 Interactions in a driven atom-cavity system

This section presents an overview of the atom-light interactions, and finally introduce the Hamiltonian for the two-mode single atom cavity QED system. We assume that we can isolate and drive one particular atomic transition and hence ignore the rest of the atomic structure. So we can approximate or model as having only two-level atoms. This approximation is applicable when the frequency of the light coincides with one of the optical transitions of the atom. In this case the internal atomic Hamiltonian H_A can be

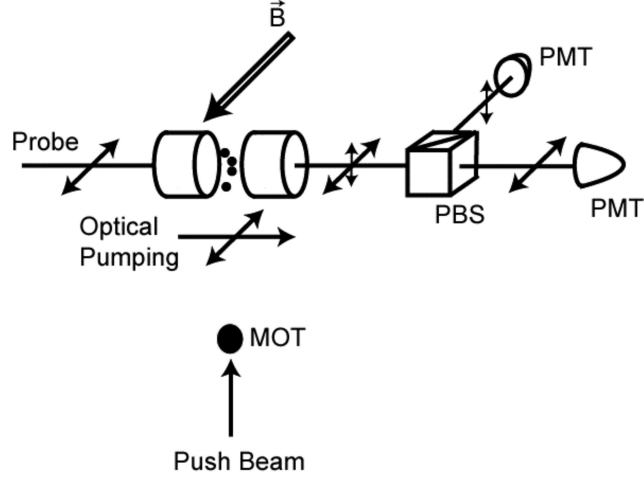


Figure 1: Taken from [7]

written as

$$H_A = E_g |g\rangle\langle g| + E_e |e\rangle\langle e| \quad (2.1)$$

Where E_g and E_e represent the ground and excited state respectively. We can express this hamiltonian in this form

$$H_A = \frac{\hbar w_a}{2} (|e\rangle\langle e| - |g\rangle\langle g|) \quad (2.2)$$

where $w_a = (E_e - E_g)/\hbar$. We have used the fact that we have set the zero of our energy scale halfway between the ground state and the excited state. This can be express more compactly

$$H_A = \frac{\hbar w_A}{2} \sigma_z \quad (2.3)$$

where

$$\sigma_z = |e\rangle\langle e| - |g\rangle\langle g| \quad (2.4)$$

The interaction of radiation field E with a single-electron atom can be describe by the following Hamiltonian in the dipole approximation

$$H = H_A + H_F - d \cdot E \quad (2.5)$$

Here H_A (see 2.2) and H_F are the energies of the atom and the radiation field, respectively, in the absence of the interaction and d is the atomic dipole moment $d = e\mathbf{r}$. In the dipole approximation, the field is assumed to be unifrom over the whole atom. The energy of

the free field H_F is given in terms of the creation and destruction operators by

$$H_F = \hbar\omega_b \hat{b}^\dagger \hat{b} \quad (2.6)$$

Upon imposing quantisation the interaction Hamiltonian becomes

$$i\hbar g(\hat{b}^\dagger - \hat{b})(\sigma_+ + \sigma_-) \quad (2.7)$$

Here g is the dipole coupling constant that takes up the normalisation constant from the electromagnetic wave and the dipole matrix element. The terms \hat{b}^\dagger and \hat{b} represent the usual raising and lowering operators. Where the atomic lowering and raising operators are define

$$\sigma_+ = |e\rangle\langle g| \quad \sigma_- = |g\rangle\langle e| \quad (2.8)$$

The interaction energy in 2.7 consists of four terms. The term $\hat{b}^\dagger \sigma_-$ describes the process in which the atom is taken from the upper state into the lower state and a photon is created. The term $\hat{b} \sigma_+$ describes the opposite process. The energy is conserved in both the proocesses. The term $\hat{a} \sigma_-$ describes a process in which the atom makes a transition from the upper to the lower level and a photon is annihilated. Similarly $\hat{b}^\dagger \sigma_+$ describes the converse process. This two latter process do not conserve energy, getting rid of this terms corresponds to the rotating-wave approximation. This results in the following Hamiltonian

$$H = H_0 + W \quad (2.9)$$

with the free Hamiltonian

$$H_0 = \frac{\hbar\omega_A}{2} \sigma_z + \hbar\omega_b \hat{b}^\dagger \hat{b} \quad (2.10)$$

and an interaction hamiltonian

$$W = \hbar g(\hat{b}^\dagger \hat{\sigma}_- - \hat{b} \hat{\sigma}_+) \quad (2.11)$$

Cavity-Laser Interactions

When the system is subject to a coherent driving laser, the Hamiltonian for this system can be expressed as:

$$H = H_0 + W_{LC} \quad (2.12)$$

with a free part for the quantised cavity mode

$$H_0 = \hbar\omega_a \hat{a}^\dagger \hat{a} \quad (2.13)$$

and an interaction part W_{LC} . If the laser frequency w_L is near resonance with a cavity mode a of frequency w_a (i.e. $w_L \approx w_a$) and assuming that the driving laser only interacts with a cavity mode with the same polarisation. Then in the rotating-wave approximation this Hamiltonian becomes

$$W_{LC} = i\hbar\mathcal{E}(\hat{a}^\dagger e^{-i\hbar w_L t} - \hat{a} e^{i\hbar w_L t}) \quad (2.14)$$

where \mathcal{E} is the coupling constant that takes normalisation constant between the laser field and the driven cavity mode.

2.3 Selection Rules

The light-matter interaction is described by transition probabilities, which can be calculated for the case of spontaneous emission by using Fermi's golden rule. According to this rule the transition rate is given by

$$P_{i \rightarrow f} = \frac{2\pi}{\hbar} |\langle \phi_f | W | \phi_i \rangle|^2 \rho(E_i) \quad (2.15)$$

where $|\phi_i\rangle$ and $|\phi_f\rangle$ are eigenstates of the unperturbed system, and $\rho(E_i)$ is the density of states.

Selection rules for hyperfine structure

The selection rules for electromagnetic dipole transitions for the hyperfine structure are

$$m_{F,f} - m_{F,i} = -1, 0, +1 \quad (2.16)$$

$$F_f - F_i = -1, 0, +1 \quad (2.17)$$

as the allowed transitions but

$$F_i = 0 \rightarrow F_f = 0 \quad (2.18)$$

$$m_{F,i} = 0 \rightarrow m_{F,f} = 0, \quad F_f - F_i = 0 \quad (2.19)$$

are forbidden.

Example. Figure 1.5 shows the allowed electric dipole transitions for an $F = 3$ to $F' = 4$ transition of the D₂-line of a ^{85}Rb -atom ($I = 5/2$).

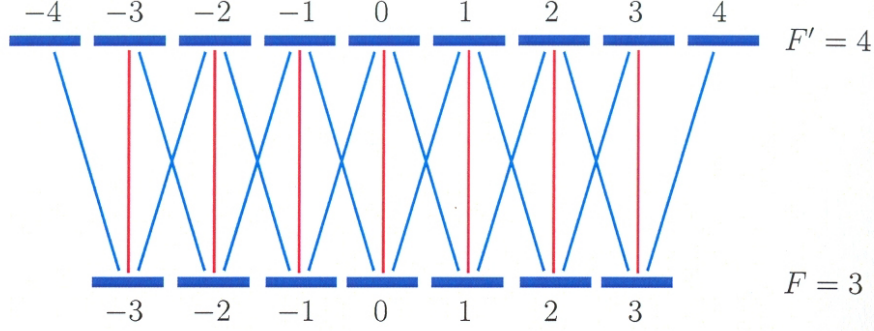


Figure 1.5 Atomic level structure and allowed electromagnetic dipole transitions for an $F = 3$ to $F' = 4$ transition. The relative transition strengths are determined by the appropriate Clebsch-Gordan coefficients. The colour coding refers to the two-mode cavity QED set-up described in section 1.1: the driven mode interacts with the atom via $\Delta m_F = 0$ transitions, and the non-driven mode via $\Delta m_F = \pm 1$ transitions.

Figure 2: taken from [3]

2.4 Hamiltonian of a driven single-atom two-mode cavity system

Now that we have presented the interaction of a single two-level atom with a single-mode field and the cavity laser interaction, we are ready to describe the system we introduce at the beginning. Assuming that the two levels of the atom are non-degenerate and the atom couples to both cavity modes, the Hamiltonian of this system can be written as

$$H = H_0 + W \quad (2.20)$$

with a free part H_0 for the two cavity modes and the atom

$$H_0 = \hbar\omega_a \hat{a}^\dagger \hat{a} + \hbar\omega_b \hat{b}^\dagger \hat{b} + \frac{\hbar\omega_a}{2} \sigma_z \quad (2.21)$$

and an interaction part

$$\begin{aligned} W = & i\hbar\mathcal{E}(\hat{a}^\dagger e^{-i\hbar\omega_L t} - \hat{a} e^{i\hbar\omega_L t}) \\ & + i\hbar g_a(\hat{a}^\dagger \hat{\sigma}_- - \hat{a} \hat{\sigma}_+) + i\hbar g_b(\hat{b}^\dagger \hat{\sigma}_- - \hat{b} \hat{\sigma}_+) \end{aligned} \quad (2.22)$$

where g_a and g_b are the coupling constants between the atom and the two cavity modes. In a frame rotating at the laser frequency the Hamiltonian becomes

$$H = \frac{\hbar(w_A - w_L)}{2} \hat{\sigma}_z + \hbar(w_a - w_L) \hat{a}^\dagger \hat{a} + \hbar(w_b - w_L) \hat{b}^\dagger \hat{b} + i\hbar\mathcal{E}(\hat{a}^\dagger - \hat{a}) + i\hbar g_a(\hat{a}^\dagger \hat{\sigma}_- - \hat{a} \hat{\sigma}_+) + i\hbar g_b(\hat{b}^\dagger \hat{\sigma}_- - \hat{b} \hat{\sigma}_+) \quad (2.23)$$

This simplifies if all frequencies are resonant, i.e. $w_L = w_a = w_b = w_A$

For a two level atom with Zeeman substructure we assume a quantisation axis, imposed by a weak magnetic field with negligible Zeeman effect, such that the driven mode a couples the atomic ground and excited state via $\Delta m_F = 0$ transitions, and the non-driven mode b couples them via $\Delta m_F = \pm 1$ transitions. Considering a resonant driven single-atom interacts on resonance with the two orthogonal linearly-polarised cavity modes. The system Hamiltonian in the dipole and rotating-wave approximation is given by

$$H = i\hbar\mathcal{E}(\hat{a}^\dagger - \hat{a}) + i\hbar g(\hat{a}^\dagger \hat{\Sigma}_0 - \hat{a} \hat{\Sigma}_0^\dagger) + i\hbar(g/\sqrt{2})(\hat{b}^\dagger(\hat{\Sigma}_{-1} + \hat{\Sigma}_{+1}) - \hat{b}(\hat{\Sigma}_{-1} + \hat{\Sigma}_{+1})^\dagger) \quad (2.24)$$

For atomic transitions with $F_g = F_e - 1$ the atomic operators are expressed as

$$\hat{\Sigma}_p = \sum_{m=-3}^3 C_{F_e, m+p, F_g, m} |F_g, m\rangle \langle F_e, m+p| \quad (2.25)$$

where p stands for $p = 0, \pm 1$ and with the Clebsch-Gordon coefficients

$$C_{F_e, m_e, F_g, m_g} = \langle F_g, m_g; 1, m_g - m_e | F_e, m_e \rangle \quad (2.26)$$

For this particular cavity QED experiment we are interested in modeling, the atomic transition $F = 3$ to $F' = 4$. The lowering and raising operator for this particular

transition are given by

$$\begin{aligned}\hat{\Sigma}_{-1} = & |g_{-3}\rangle\langle e_{-4}| + \sqrt{\frac{3}{4}}|g_{-2}\rangle\langle e_{-3}| + \sqrt{\frac{15}{28}}|g_{-1}\rangle\langle e_{-2}| + \sqrt{\frac{5}{14}}|g_{-0}\rangle\langle e_{-1}| \\ & + \sqrt{\frac{3}{14}}|g_{+1}\rangle\langle e_0| + \sqrt{\frac{3}{28}}|g_{+2}\rangle\langle e_{+1}| + \sqrt{\frac{1}{28}}|g_{+3}\rangle\langle e_{+2}| \end{aligned} \quad (2.27)$$

$$\begin{aligned}\hat{\Sigma}_0 = & \sqrt{\frac{1}{4}}|g_{-3}\rangle\langle e_{-3}| + \sqrt{\frac{3}{7}}|g_{-2}\rangle\langle e_{-2}| + \sqrt{\frac{15}{28}}|g_{-1}\rangle\langle e_{-1}| + \sqrt{\frac{16}{28}}|g_0\rangle\langle e_0| \\ & + \sqrt{\frac{15}{28}}|g_{+1}\rangle\langle e_{+1}| + \sqrt{\frac{3}{7}}|g_{+2}\rangle\langle e_{+2}| + \sqrt{\frac{1}{4}}|g_{+3}\rangle\langle e_{+3}| \end{aligned} \quad (2.28)$$

$$\begin{aligned}\hat{\Sigma}_{+1} = & \sqrt{\frac{1}{28}}|g_{-3}\rangle\langle e_{-2}| + \sqrt{\frac{3}{28}}|g_{-2}\rangle\langle e_{-1}| + \sqrt{\frac{3}{14}}|g_{-1}\rangle\langle e_0| + \sqrt{\frac{5}{14}}|g_0\rangle\langle e_{+1}| \\ & + \sqrt{\frac{15}{28}}|g_{+1}\rangle\langle e_{+2}| + \sqrt{\frac{3}{4}}|g_{+2}\rangle\langle e_{+3}| + |g_{+3}\rangle\langle e_{+4}| \end{aligned} \quad (2.29)$$

This is the Hamiltonian that describes the system of interest where the Zeeman effect can be negligible and our point of start for our project. In the next section we study how this Hamiltonian is modified when the magnetic effect induces a Zeeman effect that can no longer be treated as negligible.

3 Hamiltonian of a driven single-atom two-mode cavity system in the presence of a magnetic field

As presented in the previous chapter, the system is subject to an external magnetic field. This causes a splitting of the energies lifting the degeneracies. In this chapter we are concerned in how the magnetic field modifies the Hamiltonian presented earlier for the two-mode driven single atom cavity system.

3.1 Hyperfine structure in an external magnetic field

In the presence of an external magnetic field of strength B , the following magnetic interactions energies have to be considered:

$$H_{hf} = AI \cdot J \quad H_z = g_j \frac{\mu_B}{\hbar} BJ - g_I \frac{\mu_N}{\hbar} BI \quad (3.1)$$

Where A is the hyperfine constant, $g_j = 1 + \frac{J(J+1) - L(L+1) + S(S+1)}{2J(J+1)}$ is the Landé factor, μ_B is the Bohr magneton, μ_N is the nuclear magneton and I is the nuclear spin and g_I is the nuclear g factor. If the external field is so small that the magnetic potential energy of the atom in it is small compared to the energetic separation of the hyperfine terms, one speaks of the Zeeman effect of the hyperfine structure. In other words the case when $H_z \ll H_{hf}$ we only considered the H_z as a perturbation, the atom is in an eigenstate of \mathbf{F}^2 , \mathbf{J}^2 , \mathbf{I}^2 and F_z so the energy shift is given by.

$$\Delta E_B = \langle FJM_F | H_z | FJM_F \rangle \quad (3.2)$$

If we choose the magnetic field B applied along the z -axis.

$$H_z = g_j \frac{\mu_B}{\hbar} BJ_z - g_p \frac{\mu_N}{\hbar} BI_z \quad (3.3)$$

In order to calculate this energy shift we will use the vector model. The "vector" \mathbf{F} is a constant of the motion, while \mathbf{I} and \mathbf{J} are not. These vectors each have a fixed length, so that they precess about the direction of \mathbf{F} (3.1). The components of \mathbf{J} and \mathbf{I} along \mathbf{F} are fixed, while the other components, rotating as they do about the \mathbf{F} axis, average to

zero. This leads to the rule

$$J \rightarrow F \frac{(J \cdot F)}{F^2} = F \frac{(J \cdot F)}{\hbar^2 F(F+1)} \quad (3.4)$$

$$I \rightarrow F \frac{(I \cdot F)}{F^2} = F \frac{(I \cdot F)}{\hbar^2 F(F+1)} \quad (3.5)$$

In the evaluation of $\langle J_z \rangle$ and $\langle I_z \rangle$ we therefore need to calculate $\mathbf{J} \cdot \mathbf{F}$ and $\mathbf{I} \cdot \mathbf{F}$, this is easily done using $\mathbf{I} = \mathbf{F} - \mathbf{J}$ and $\mathbf{J} = \mathbf{F} - \mathbf{I}$

$$\mathbf{J} \cdot \mathbf{F} = \frac{1}{2}[\mathbf{F}^2 + \mathbf{J}^2 - \mathbf{I}^2] = \frac{\hbar^2}{2}[F(F+1) + J(J+1) - I(I+1)] \quad (3.6)$$

$$\mathbf{I} \cdot \mathbf{F} = \frac{1}{2}[\mathbf{F}^2 + \mathbf{I}^2 - \mathbf{J}^2] = \frac{\hbar^2}{2}[F(F+1) + I(I+1) - J(J+1)] \quad (3.7)$$

We simply replace $\langle J_z \rangle$ and $\langle I_z \rangle$ by respectively

$$\langle F_z \rangle \frac{F(F+1) + J(J+1) - I(I+1)}{2F(F+1)} \quad (3.8)$$

$$\langle F_z \rangle \frac{F(F+1) + I(I+1) - J(J+1)}{2F(F+1)} \quad (3.9)$$

Adding the two terms yields

$$\Delta E_B = m_F g_F \mu_B B \quad (3.10)$$

where g_F is the Landé factor given by

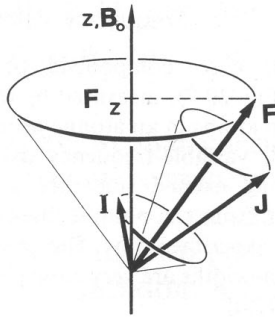


Fig. Hyperfine structure in a magnetic field. The vector diagram illustrates the Zeeman effect: the total angular momentum F , composed of the angular momentum vectors J and I , possesses quantised orientations relative to an applied magnetic field B_0 . Only the z component of F is observable

Figure 3: Taken from Haken [2]

$$g_F = g_j \left(\frac{F(F+1) + J(J+1) - I(I+1)}{2F(F+1)} \right) - g_I \frac{\mu_N}{\mu_B} \left(\frac{F(F+1) + I(I+1) - J(J+1)}{2F(F+1)} \right) \quad (3.11)$$

The second term can be neglected relative to the first term because of the factor $\mu_N/\mu_B = 1/1836$. This means that magnetic interaction due to proton spin are very weak. The term splitting in a weak field then yields $2F+1$ equidistant components, which are given by the quantum number m_F . For the optical transitions the selection rules $\Delta F = 0$ and $\Delta m = 0, \pm 1$ apply. As a final comment, when we stated a weak field, we meant a field below $0.1T$, the experiments are perform with magnetic fields below 10 G.

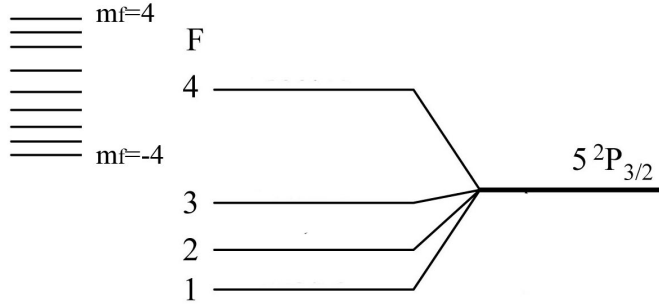


Figure 4: Example of the Zeeman splitting in the hyperfine structure for the $F=4$

3.2 Hamiltonian

Now that we know how a weak field acts on the energy levels, we incorporate them to the Hamiltonian, where the energy levels are no longer degenerate. We start from

$$H = H_0 + W \quad (3.12)$$

With a free part H_0 for the two mode cavity atom

$$H_0 = \hbar\omega_a \hat{a}^\dagger \hat{a} + \hbar\omega_b \hat{b}^\dagger \hat{b} + \sum_{m=-4}^4 E_{e,m} |e, m\rangle \langle e, m| + \sum_{m=-3}^3 E_{g,m} |g, m\rangle \langle g, m| \quad (3.13)$$

We change the term in from σ_z the sum of the different excited states and ground states. This is due to the fact that the excited states and ground state are no longer the same.

We have 9 excited states and 7 ground states. And an interaction part

$$W = i\hbar\mathcal{E}(\hat{a}^\dagger e^{-i\omega_L t} - \hat{a} e^{i\omega_L t}) + i\hbar g(\hat{a}^\dagger \hat{\Sigma}_0 - \hat{a} \hat{\Sigma}_0^\dagger) + i\hbar(g/\sqrt{2})\left(\hat{b}^\dagger(\hat{\Sigma}_{-1} + \hat{\Sigma}_{+1}) - \hat{b}(\hat{\Sigma}_{-1}^\dagger + \hat{\Sigma}_{+1}^\dagger)\right) \quad (3.14)$$

Where the terms $E_{e,m}$ and $E_{g,m}$ correspond to

$$E_{a,m} = E_{a,0} + g_{Fa}\mu_B B m \quad (3.15)$$

Where $a = e, g$ and g_{Fa} represents the Landé g factor for either e or g. Now if we refer the atomic energies to the middle of the atomic transition, as in 5 the energies of the

Atomic structure of Rb atoms. in an external magnetic field

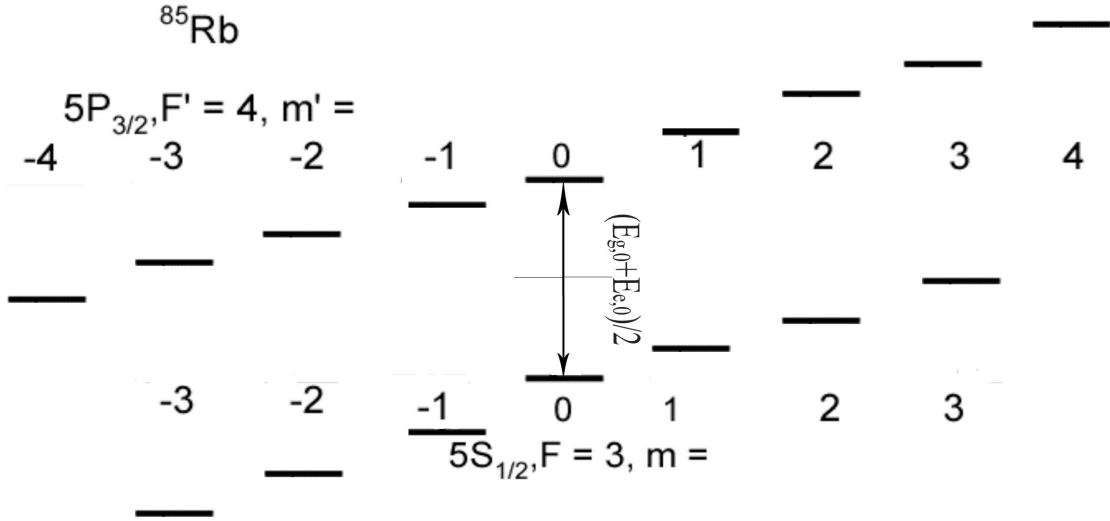


Figure 5: Shifting for the energy levels for the levels $5P_{3/2}$ and $5S_{1/2}$

two level atom may be written as

$$\sum_{m=-4}^4 \left[E_{e,m} - \frac{(E_{e,0} + E_{g,0})}{2} + \frac{(E_{e,0} + E_{g,0})}{2} \right] |e, m\rangle \langle e, m| \quad (3.16)$$

$$\sum_{m=-3}^3 \left[E_{g,m} - \frac{(E_{e,0} + E_{g,0})}{2} + \frac{(E_{e,0} + E_{g,0})}{2} \right] |g, m\rangle \langle g, m| \quad (3.17)$$

The last term is a constant which may be eliminated by the way we define the transition. We introduce a Hamiltonian of the form

$$H_L = \hbar w_L \hat{a}^\dagger \hat{a} + \hbar w_L \hat{b}^\dagger \hat{b} + \sum_{m=-4}^4 \frac{\hbar w_L}{2} |e, m\rangle \langle e, m| - \sum_{m=-3}^3 \frac{\hbar w_L}{2} |g, m\rangle \langle g, m| \quad (3.18)$$

where w_L correspond to the laser frequency. We can define an interaction Hamiltonian of the form

$$H_I = H_0 - H_L + W \quad (3.19)$$

$$H = H_L + H_I \quad (3.20)$$

We transform this to the interaction picture in order to get rid of the oscillating terms.

$$e^{i\frac{H_L t}{\hbar}} H_I e^{-i\frac{H_L t}{\hbar}} \quad (3.21)$$

We obtain

$$e^{i\frac{H_L t}{\hbar}} \hat{a} e^{-i\frac{H_L t}{\hbar}} = \hat{a} e^{-i w_L t} \quad (3.22)$$

$$e^{i w_L \frac{H_L t}{\hbar}} \hat{a}^\dagger e^{-i w_L \frac{H_L t}{\hbar}} = \hat{a}^\dagger e^{i w_L t} \quad (3.23)$$

$$e^{i w_L \frac{H_L t}{\hbar}} \hat{b} e^{-i w_L \frac{H_L t}{\hbar}} = \hat{b} e^{-i w_L t} \quad (3.24)$$

$$e^{i w_L \frac{H_L t}{\hbar}} \hat{b}^\dagger e^{-i w_L \frac{H_L t}{\hbar}} = \hat{b}^\dagger e^{i w_L t} \quad (3.25)$$

$$e^{i w_L \frac{H_L t}{\hbar}} \hat{\Sigma}_0 e^{-i w_L \frac{H_L t}{\hbar}} = \hat{\Sigma}_0 e^{-i w_L t} \quad (3.26)$$

$$e^{i w_L \frac{H_L t}{\hbar}} \hat{\Sigma}_0^\dagger e^{-i w_L \frac{H_L t}{\hbar}} = \hat{\Sigma}_0^\dagger e^{i w_L t} \quad (3.27)$$

So this reduces to

$$\begin{aligned} H = & \hbar(w_a - w_L) \hat{a}^\dagger \hat{a} + \hbar(w_b - w_L) \hat{b}^\dagger \hat{b} + \sum_{m=-4}^4 \left[\hbar \frac{(w_A - w_L)}{2} + g_F m \mu_B B \right] |e, m\rangle \langle e, m| \\ & - \sum_{m=-3}^3 \left[\hbar \frac{(w_A - w_L)}{2} - g_F m \mu_B B \right] |g, m\rangle \langle g, m| + i \hbar \mathcal{E} (\hat{a}^\dagger - \hat{a}) + i \hbar g (\hat{a}^\dagger \hat{\Sigma}_0 - \hat{a} \hat{\Sigma}_0^\dagger) \\ & + i \hbar (g/\sqrt{2}) \left(\hat{b}^\dagger (\hat{\Sigma}_{-1} + \hat{\Sigma}_{+1}) - \hat{b} (\hat{\Sigma}_{-1}^\dagger + \hat{\Sigma}_{+1}^\dagger) \right) \end{aligned} \quad (3.28)$$

Where $w_A = (E_{e,0} - E_{g,0})/\hbar$. This simplifies if all frequencies are near resonance, i.e. $w_L = w_a = w_A = w_b$ and reduces to

$$\begin{aligned}
H = & \sum_{m=-4}^4 g_{Fe} m \mu_B B |e, m\rangle \langle e, m| + \sum_{m=-3}^3 g_{Fg} m \mu_B B |g, m\rangle \langle g, m| + i\hbar \mathcal{E}(\hat{a}^\dagger - \hat{a}) \\
& + g(\hat{a}^\dagger \hat{\Sigma}_0 - \hat{a} \hat{\Sigma}_0^\dagger) + i\hbar(g/\sqrt{2}) \left(\hat{b}^\dagger (\hat{\Sigma}_{-1} + \hat{\Sigma}_{+1}) - \hat{b} (\hat{\Sigma}_{-1}^\dagger + \hat{\Sigma}_{+1}^\dagger) \right) \quad (3.29)
\end{aligned}$$

This is the Hamiltonian of a driven single-atom two-mode cavity system in the presence of a weak external magnetic field. The shifting produce by the Zeeman effect introduces some detunings into the Hamiltonian.

4 Open Quantum Systems

An open quantum system is a quantum mechanical system that interacts with an external quantum system, the environment. Since the environment is composed of a large number of degrees of freedom, we refer it to the reservoir R . Hence, an open quantum system S can be seen as a distinguishable part of a closed quantum system $S \otimes R$.

Due to the dissipative nature of an open quantum system one generally does not have a complete knowledge of the system state. Therefore, the system cannot be describe by a state vector, rather, is describe by its density operator. In this section we will present two well establissed tools to study this dissipation or damping: namely the master equation and the quantum trajectory approach.

4.1 The Master Equation approach

We begin from von Neumann's equation for the density operator $\chi(t)$

$$\dot{\chi}(t) = \frac{1}{i\hbar}[H, \chi(t)] \quad (4.1)$$

We assume we can divide the closed system into two pieces: a system which we are interested in, and the environment or reservoir that interacts with the system. Accordingly we may write the Hamiltonian for this composite system as.

$$H = H_S + H_R + H_{SR} \quad (4.2)$$

where H_S is ty system Hamiltonian, H_R is the reservoir Hamilltonian and H_{SR} is an interaction Hamiltonian between the system and the reservoir. We transform to the interaction picture in order to separated the rapid oscillation genearted by $H_S + H_R$ from the slow motion generated by the interaction H_{SR} .

$$\tilde{\chi}(t) = e^{i(H_S+H_R)t/\hbar} \chi(t) e^{-i(H_S+H_R)t/\hbar} \quad (4.3)$$

$$\tilde{H}_{SR}(t) = e^{i(H_S+H_R)t/\hbar} H_{SR}(t) e^{-i(H_S+H_R)t/\hbar} \quad (4.4)$$

The equation of motion for the density operator is now

$$\dot{\tilde{\chi}}(t) = \frac{1}{i\hbar}[\tilde{H}_{SR}(t), \tilde{\chi}(t)] \quad (4.5)$$

We can now integrate formally to give

$$\tilde{\chi}(t) = \tilde{\chi}(0) + \frac{1}{i\hbar} \int_0^t ds [\tilde{H}_{SR}(t), [\tilde{H}_{SR}(t-s), \tilde{\chi}(t-s)]] \quad (4.6)$$

and substitute for $\tilde{\chi}(t)$ inside the commutator in to eg(4.6)

$$\dot{\tilde{\chi}}(t) = \frac{1}{i\hbar} [\tilde{H}_{SR}(t), \tilde{\chi}(0)] - \frac{1}{\hbar^2} \int_0^t ds [\tilde{H}_{SR}(t), [\tilde{H}_{SR}(t-s), \tilde{\chi}(t-s)]] \quad (4.7)$$

This equation is no exactly solvable. Nevertheless, it is possible to proceed and construct an equation of motion for the reduce density operator.

The Born-Markov Approximation

We are interested in describing the sytem S and we are not interested in detailed information about the reservoir R. Thus is convinient to introduce the reduced density operator describing S by taking a partial trace over the reservoir variables of the density operator for the composite system.

$$\rho(t) = tr_R\{\chi(t)\} \quad (4.8)$$

We assume the density operator is initially in a factorised state

$$\tilde{\chi}(0) = R_0 \tilde{\rho}(0) \quad (4.9)$$

where $\rho(0)$ is the intial system density operator and R_0 is the equilibrium reservoir desntiy operator at time $t = 0$ when we turn the interaction between the system and its environ-ment. Deviations from the direct product come from the interaction. If the interaction is very weak we expect that at all times $\tilde{\chi}(t)$ deviates from an uncorrelated state in first or higher oder of H_{SR} .

$$\tilde{\chi}(t) = R_0 \tilde{\rho}(t) + \mathcal{O}(H_{SR}) \quad (4.10)$$

Since the first term is the dominant contribution we only retain this leading order term, thus introducing a Born Approximation.

The next assumption introduced is Markov assummption, where we assume that the system's future behaviour depnds only on its current state, rather than its histroy. This assumption is justified if there ar two widely spearted timescales: a short reservoir correlation time and the longer timescale that the systems changes over. If the reservoir correlation time is much smaller than the time scale of correlated fluctuactions in the system S we may replace $\tilde{\rho}(t-s)$ by $\tilde{\rho}(t)$ in the master equation. Also for times s much

larger than the reservoir correlation time the integrand of the master equation vanishes, so we can extend the upper limit to infinity. We obtain the master equation in the Born-Markov approximation:

$$\dot{\tilde{\rho}}(t) = -\frac{1}{\hbar^2} \int_0^\infty ds \text{tr}_R \left\{ \left[\tilde{H}_{SR}(t), \left[\tilde{H}_{SR}(t-s), R_0 \tilde{\rho}(t-s) \right] \right] \right\} \quad (4.11)$$

General Lindblad master equation

If we expand the interaction Hamiltonian in terms of eigenoperators of the system Hamiltonian

$$H_{SR} = \hbar \sum_{i,j,k} \kappa_{ijk} \hat{A}_{ij} \hat{\Gamma}_k \quad (4.12)$$

where $\hat{\Gamma}_k$ are independent reservoir operators and \hat{A}_{ij} are degenerate eigenoperators of H_S such that

$$[\hat{A}_{ij}, H_S] = \hbar w_i \hat{A}_{ij} \quad (4.13)$$

Substituting equation 4.12 in the interaction picture into the Born-Markov approximation 4.11; and taking into consideration that in optical systems oscillations on a much smaller time-scale than the relaxation time of the system. This allowed us that upon integration of the master equation over an interval that is much longer than the period of oscillation, these terms will tend to average out. Following this procedure one is able to find the master equation in Lindblad form

$$\dot{\rho} = \frac{1}{i\hbar} [H'_S, \rho(t)] + \sum_i \frac{\gamma_i}{2} \left(2\hat{A}_i \rho(t) \hat{A}_i^\dagger - \hat{A}_i^\dagger \hat{A}_i \rho(t) - \rho(t) \hat{A}_i^\dagger \hat{A}_i \right) \quad (4.14)$$

The terms $-\hat{A}_i^\dagger \hat{A}_i \rho(t)$ and $-\rho(t) \hat{A}_i^\dagger \hat{A}_i$ in the Lindblad form of the master equation describe the loss of population from the current states, whereas the terms $\hat{A}_i \rho(t) \hat{A}_i^\dagger$ describe the gain of population of the states toward which the system propagates.

In preparation for the quantum trajectory, it is useful to rewrite the master equation for the reduced density operator in a more abstract notation

$$\dot{\rho}(t) = \mathcal{L}\rho(t) \quad (4.15)$$

\mathcal{L} is a generalised Liouvillian superoperator. It is a linear operator that acts on operators rather than on vectors in the Hilbert space. In the case for the master equation in Lindblad form the action of \mathcal{L} is defined as

$$\mathcal{L} \cdot = \frac{1}{i\hbar} [H'_S, \cdot] + \sum_i \frac{\gamma_i}{2} (2\hat{A}_i \cdot \hat{A}_i^\dagger - \hat{A}_i^\dagger \hat{A}_i \cdot - \cdot \hat{A}_i^\dagger \hat{A}_i) \quad (4.16)$$

4.2 Quantum Trajectory approach

We start from the master equation of the form

$$\dot{\rho}(t) = (\mathcal{L}_0 + S)\rho(t) \quad (4.17)$$

with

$$\mathcal{L}_0 = \mathcal{L} - S \quad (4.18)$$

The formal solution is

$$\rho(t) = e^{(\mathcal{L}_0 + S)t} \rho(0) \quad (4.19)$$

provided that $(\mathcal{L}_0 + S)$ is not explicitly time-dependant. We define an auxiliary density operator

$$\rho'(t) = e^{-\mathcal{L}_0 t} \rho(0) \quad (4.20)$$

If we take the time-derivative of equation 4.20 and using equation 4.17 leads to the equation of motion for $\rho'(t)$

$$\dot{\rho}'(t) = e^{-\mathcal{L}_0 t} \mathcal{S} e^{\mathcal{L}_0 t} \rho'(t) \quad (4.21)$$

If we formally integrate this equation, use equation 4.20 and multiply by $e^{\mathcal{L}t}$ from the right, which now reads as

$$\rho(t) = \rho(0) + \int_0^t ds e^{\mathcal{L}_0(t-s)} \mathcal{S} e^{\mathcal{L}_0 s} \rho'(s) \quad (4.22)$$

Iterating this solution into itself we find

$$\rho(t) = \sum_{m=0}^{\infty} \int_0^t dt_m \int_0^{t_m} dt_{m-1} \dots \int_0^{t_2} dt_1 e^{\mathcal{L}_0(t-t_m)} \mathcal{S} e^{\mathcal{L}_0(t_m-t_{m-1})} \mathcal{S} \dots \mathcal{S} e^{\mathcal{L}_0 t_1} \rho(0) \quad (4.23)$$

This is a Dyson's series, where (t_m) is a monotonic increasing sequence. The integration kernel describes a quantum trajectory of the initial state $\rho(0)$. The terms $e^{\mathcal{L}_0(t_m-t_{m-1})}$ represent a continuous time-evolution in the time interval $[t_m, t_{m-1}]$ and \mathcal{S} represents discontinuous collapses at the times t_1, t_2, \dots, t_m . Equation 4.23 is simply the sum over all possible numbers of collapses, $m = 0, \dots, \infty$ and an integration over all possible separation times of these emissions within the interval $[0, t]$.

The solution of the master equation, when we take distinguishable perturbations into

account each causing the system to collapse at different times, takes the form

$$\dot{\rho} = (\mathcal{L}_0 + \mathcal{S})\rho \quad \text{with} \quad \mathcal{S} = \sum_i \mathcal{S}_i \quad (4.24)$$

where \mathcal{S} is a small perturbation of \mathcal{L}_0 is

$$\begin{aligned} \rho(t) = & \sum_{\nu_1=1}^{\infty} \sum_{\nu_1=1}^I \sum_{\nu_2=2}^I \cdots \sum_{\nu_m=1}^I \int_0^t dt_m \int_0^{t_m} dt_{m-1} \cdots \int_0^{t_2} dt_1 e^{\mathcal{L}_0(t-t_m)} \mathcal{S}_{\nu_m} \\ & \times e^{\mathcal{L}_0(t_m-t_{m-1})} \mathcal{S}_{\nu_{m-1}} \cdots \mathcal{S}_{\nu_1} e^{\mathcal{L}_0 t_1} \rho(0) \end{aligned} \quad (4.25)$$

The integration kernel describes a quantum trajectory of the initial state $\rho(0)$, and the equation is simply the summation over all possible trajectories.

We introduce the conditioned reduce density operator $\rho_c(t)$ describing the system at time t with initial state $\rho(0)$ and a particular sequence of collapse times in the interval $[0, t]$

$$\rho_c(t) = \frac{\bar{\rho}_c(t)}{\text{tr}\{\bar{\rho}_c(t)\}} \quad (4.26)$$

where $\bar{\rho}_c(t)$ is the unnormalised operator

$$\bar{\rho}_c(t) = e^{\mathcal{L}_0(t-t_m)} \mathcal{S}_{\nu_m} e^{\mathcal{L}_0(t_m-t_{m-1})} \mathcal{S}_{\nu_{m-1}} \cdots \mathcal{S}_{\nu_1} e^{\mathcal{L}_0 t_1} \rho(0) \quad (4.27)$$

It is possible to rewrite the master equation in Lindblad form

$$\dot{\rho}(t) = (\mathcal{L}_0 + \mathcal{S})\rho \quad \text{with} \quad \mathcal{S} = \sum_i \mathcal{S}_i \quad (4.28)$$

with

$$\mathcal{L}_0 = \frac{1}{i\hbar} [H'_s, \rho] - \sum_i \frac{\gamma_i}{2} (A_i^\dagger A_i \rho + \rho A_i^\dagger) = \frac{1}{i\hbar} (H_{eff} \rho - \rho H_{eff}) \quad (4.29)$$

$$\mathcal{S}_i \rho = \gamma_i A_i \rho A_i^\dagger = C_i \rho C_i^\dagger \quad (4.30)$$

where we have introduced the collapse operators

$$C_i = \sqrt{\gamma_i} A_i \quad (4.31)$$

and H_{eff} is an effective, non-Hermitian Hamiltonian define as

$$H_{eff} = H'_S - \sum_i \gamma_i A_i \rho A_i^\dagger \quad (4.32)$$

Often the conditioned density operator can be factorised in a pure state at time t

$$\rho_c(t) = |\psi_c(t)\rangle\langle\psi_c(t)| \quad (4.33)$$

If a system starts a pure state, then under time evolution, it will remain in a pure state. This is one of the advantages to the quantum jump approach. It allows us to replace the propagators $e^{(\mathcal{L}-\mathcal{S})t}$ with propagators for the state vector $e^{-iH_{eff}t/\hbar}$ and at times of collapses we have $\hat{C}_i|\bar{\psi}\rangle$.

Monte Carlo Recipe

1. Calculate the probabilities $p_{c,i}(t_n)$ for a collapse in the interval $[t_n, t_n + \Delta t]$

$$p_{c,i}(t_n) = \langle\psi_c(t_n)|\hat{C}_i^\dagger\hat{C}_i|\psi_c(t_n)\rangle\Delta t \quad (4.34)$$

2. Choose whether a jump occurs or not. If it does occur, choose randomly the corresponding jump operator \hat{C}_j . Both choices are performed by drawing a single random value r , chosen between 0 and 1. If a jump occur, its index j is the smallest integer such that $\sum_i^j p_{c,i}(t_n) > r$.
3. In the no jump case, compute the elementary evolution of $|\psi_c(t_n)\rangle$ under the effective non-hermitian Hamiltonian. Renormalize the final result to get the new state.
4. In the event of a jump, compute the new state and renormalize it.
5. Repeat the sequence of steps with the resulting state $|\bar{\psi}_c(t_{n+1})\rangle$ as a new initial state.

It is important to note that that the Linbland and Monte Carlo approaches are fully equivalent. The quantum monte carlo approach is better suited for computational simulations, especially for modelling systems with a large number of N of possible states. The computational advantage of the monte-carlo algorithm is that the time evolution of the system involves solving a set of only $\mathcal{O}(N)$ differential equations, as opposed to $\mathcal{O}(N^2)$ required when solving the master equation directly.

5 Numerical simulations: 2-mode cavity QED

Now that we have presented the formal apparatus to study this type of systems. In this section we present the results from the numerical simulation of the sytem presented in section two. Using the two methods presented in section three. First we show the properties from the master equation and later compared it with the quantum trajectory method.

5.1 Master Equation

In order to avoid accuracy problems due to different order of magnitude, we will work with a master equation such that all terms are of a similar order of magnitude. A dimensionless master equation:

$$\begin{aligned} \frac{d\rho(t)}{d(\kappa t)} = & \left[\frac{H_S}{i\hbar\kappa} \right] + (2\hat{a}\rho(t)\hat{a}^\dagger - \hat{a}^\dagger\hat{a}\rho(t) - \rho(t)\hat{a}^\dagger\hat{a}) \\ & + (2\hat{b}\rho(t)\hat{b}^\dagger - \hat{b}^\dagger\hat{b}\rho(t) - \rho(t)\hat{b}^\dagger\hat{b}) \\ & + \frac{\gamma}{2\kappa} \sum_{p=0,\pm 1} \left(2\hat{\Sigma}_p\rho(t)\hat{\Sigma}_p^\dagger - \hat{\Sigma}_p^\dagger\hat{\Sigma}_p - \rho(t)\hat{\Sigma}_p^\dagger\hat{\Sigma}_p \right) \end{aligned} \quad (5.1)$$

with

$$\begin{aligned} \frac{H_S}{i\hbar\kappa} = & \sum_{m=-4}^4 \frac{g_{F_e}Be}{2m_e\kappa} |e, m\rangle\langle e, m| + \sum_{m=-3}^3 \frac{g_{F_g}Be}{2m_e\kappa} |g, m\rangle\langle g, m| + \frac{\mathcal{E}}{\kappa}(\hat{a}^\dagger - \hat{a}) \\ & + \frac{g}{\kappa}(\hat{a}^\dagger\hat{\Sigma}_0 - \hat{a}\hat{\Sigma}_0) + \frac{g}{\kappa} \left(\hat{b}^\dagger \frac{(\hat{\Sigma}_{-1} + \hat{\Sigma}_{+1})}{\sqrt{2}} - \hat{b} \frac{(\hat{\Sigma}_{-1} + \hat{\Sigma}_{+1})^\dagger}{\sqrt{2}} \right) \end{aligned} \quad (5.2)$$

Fock Space Truncation

Its a good approximation to neglect all Fock states with a photon number larger than N_α , to truncate the Fock space of the cavity mode α . If N_a and N_b are the maximum considered numbers of photons in the driven and non-driven cavity modes, respectively, the Hilbert space \mathcal{H} of our atom cavity system with truncated Fock spaces for the cavity mode.

$$H = H_{atom} \otimes H_{drivenmode} \otimes H_{non-drivenmode} \quad (5.3)$$

Steady State Properties

Mean photon number of the cavity modes

Figure 6 shows the mean photon numbers of the driven and non-driven cavity mode, given by:

$$\langle \hat{\nu}^\dagger \hat{\nu} \rangle = Tr_s \{ \hat{\nu}^\dagger \hat{\nu} \rho_{ss} \} \quad (5.4)$$

where $\hat{\nu} = \hat{a}, \hat{b}$, for varying dipole coupling and driving strengths. We observe that, the mean photon number in the driven mode is larger than that in the non-driven mode.

Dipole coupling strength variation

When the dipole coupling strength is switched on and increased, we noticed two effects, the first effect is due to the coupling between the atom and the cavity modes, the atom can be excited. As a consequence photons are scattered from the driven mode into both the non-driven mode and the free space. Secondly the magnitude of the vacuum Rabi splitting increase with increasing coupling strength. These leads to a decrease in the mean photon number in the driven mode when the coupling strength is increased. Their is a difference between the case of no field and field case, in the no field case the mean photon number tends to zero. For the field on case the mean photon number reduces to a minimum.

For the mean photon in the non-driven mode, these effects have opposite character. All the photons in the non-driven mode originate from emission events of the atom. This yields an initial increase in the mean photon number when the dipole coupling strength is increased. For larger coupling, tends to achieve a constant mean photon number.

Driving field strenght variation

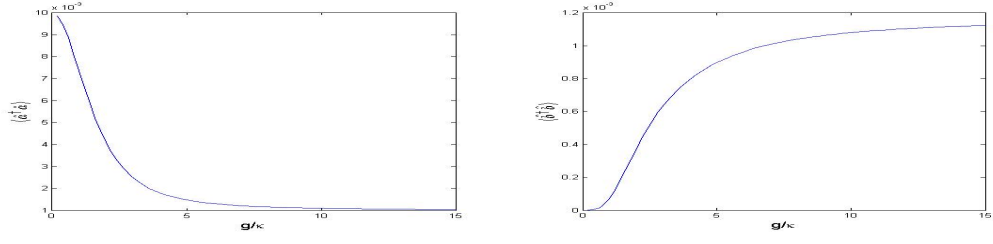
If the strength of the driving field is inscreased, more photons are provided by the laser. Therefore the mean photon number in the driven mode increases. With a large average photon number in the driven mode, more photons are scattered into the non-driven mode.

Field amplitude of the driven mode

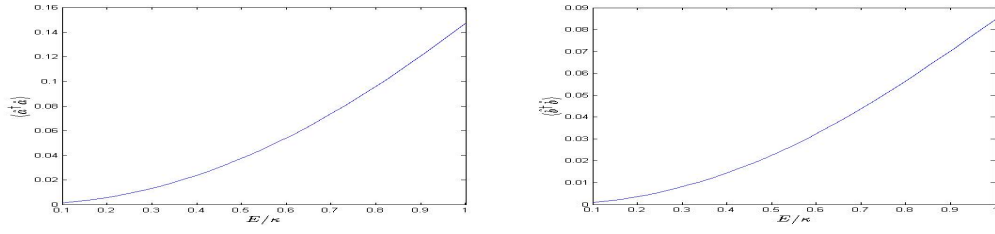
As a second steady state property we calculate the mean amplitude of the driven mode

$$\langle \hat{a} \rangle = Tr_s \{ \hat{a} \rho_{ss} \} \quad (5.5)$$

for varying coupling and dirving field strengths(see figure 7). The amplitude of the driven mode has a coherent part from the driving field and an incoherent part from the interaction with the atom. Since the coherent part does not average out, the amplitude of the driven mode has a non-zero mean. On the other hand, the mean amplitude of the non-driven cavity mode is zero.

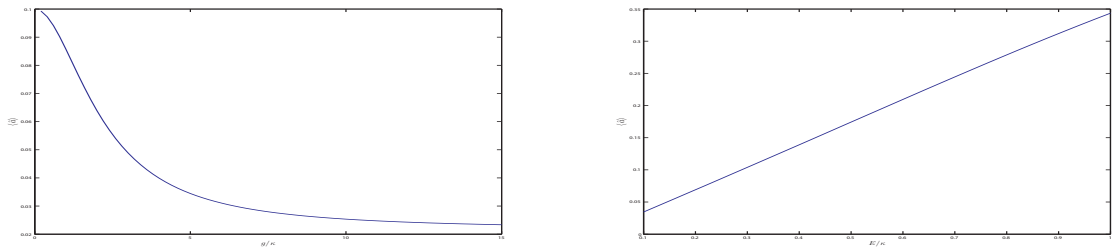


(a)



(b)

Figure 6: Mean photon numbers of the driven and non-driven cavity modes for $\gamma/\kappa = 6$, and (a) $\mathcal{E}/\kappa = 0.1$ and varying coupling constant g , (b) $g/\kappa = 5$ and varying driving field strength E .



(a)

(b)

Figure 7: Mean field amplitude of the driven cavity mode for $\gamma/\kappa = 6$ and $\mathcal{E}/\kappa = 0.1$ and varying coupling constant g , (b) $g/\kappa = 5$ and varying driving strength E

Second-order photon correlation function

We calculate the second order photon correlation function according to

$$g_{\mu\nu}^{(2)}(\tau) = \frac{\langle \hat{\mu}^\dagger(0) \hat{\nu}^\dagger(\tau) \hat{\nu}(\tau) \hat{\mu}(0) \rangle_{ss}}{\langle \hat{\mu}^\dagger \hat{\mu} \rangle_{ss} \langle \hat{\nu}^\dagger \hat{\nu} \rangle_{ss}} \quad (5.6)$$

The correlation functions for an illustrative set of parameters are shown in figure 9. The magnetic field induces an oscillation to the second order correlation at the Lamor frequency. We noticed from the simulation, that for weak drivin field the oscillations remain for long time and as the driving field becomes stronger the oscillations diminish. This is, at least qualitatively, what is reported by Orozcos group see figure 8. They also report that a transition to a strong drive causes oscillation to disappear. The breakdown of detailed balance for the two-mode cross-correlation that is observed in the absence of the magnetic field; persists when the magnetic field is turn on.

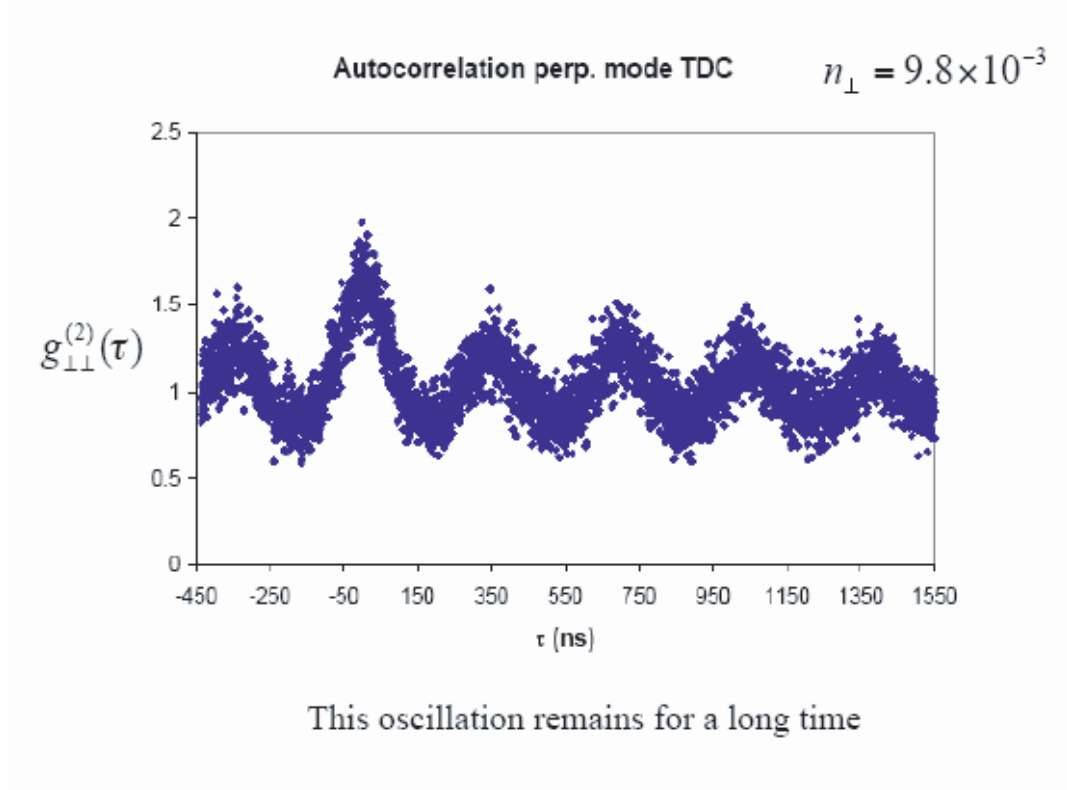


Figure 8: Taken from [4]

As we increase the strength of the driving field, the mean photon number in the cavity would increase as well, and our chosen truncation of the Fock space would become a bad approximation. However the master equation is not suited to handle larger Fock spaces,

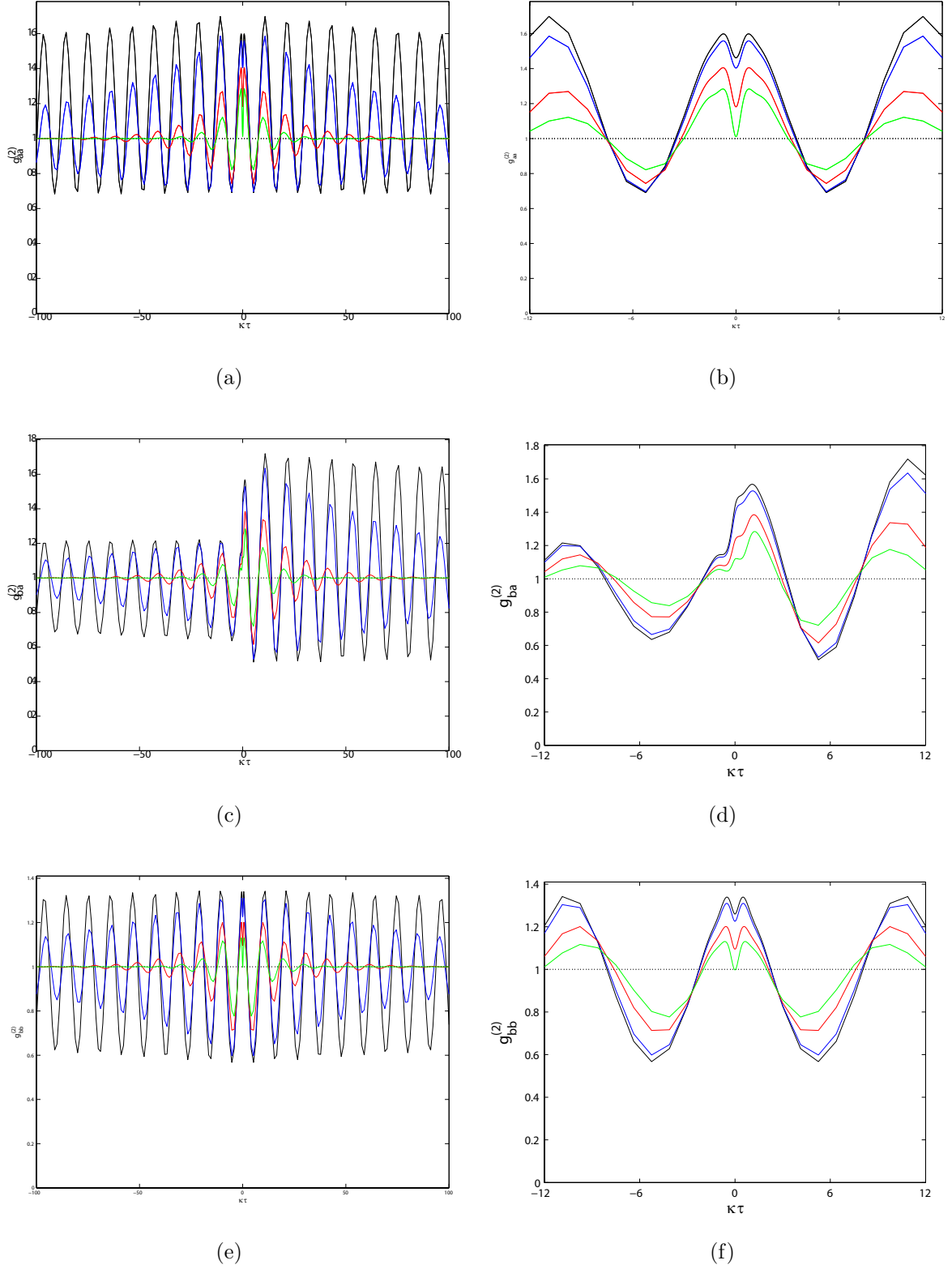


Figure 9: Steady state second-order photon correlation functions for $\gamma/\kappa = 6, g/\kappa = 5$, and $\mathcal{E}/\kappa = 0.1, 0.3, 0.7$, and 1.0 and $B = 1 \times 10^{-5}$ T: (a) and (b) driven mode self-correlation, (c) and (d) two-mode cross-correlation, and (e) and (f) non-driven mode self-correlation. Each correlation function is plotted twice, for a large time scale on the left hand side, and for short time scale on the right hand side.

because we have to solve $\mathcal{O}(N^2)$ equations, so we find computational difficulties. For larger driving field strengths, we therefore use a quantum trajectory approach, that is better suited for larger Fock spaces.

5.2 Quantum Trajectory

The numerical integration of the master equation revealed the behaviour of the system when is subject to a weak external magnetic field. In this section, we explore driving field strength away from the weak excitation regime, using a simulation of our system based on quantum trajectory theory.

The considered two-mode cavity QED system radiates five fields: The cavity radiates two fields, one for each cavity mode, which are transmitted through the cavity output mirrors. Three fields of different polarisations are radiated out the side of the cavity by atomic spontaneous emission. The system is initailly prepared in a pure state(the atom in the $m_F = 0$ ground state and no photons in the non-driven mode), this results in a non-unitary time evolution for the conditioned system wavefunction:

$$|\bar{\psi}_c(\kappa t + \Delta(\kappa t))\rangle = e^{\frac{iH_{eff}}{\kappa\hbar}\Delta(\kappa t)}|\bar{\psi}_c(\kappa t)\rangle \quad (5.7)$$

with

$$\frac{iH_{eff}}{\kappa\hbar} = -\frac{H_S}{i\hbar\kappa} + \sum_{\nu=a,b} \hat{\nu}^\dagger \hat{\nu} + \frac{\gamma}{2\kappa} \sum_{p=0,\pm 1} \hat{\Sigma}_p^\dagger \hat{\Sigma}_p \quad (5.8)$$

where $\frac{H_S}{i\hbar\kappa}$ is given by equation 5.2. The coherent time evolution of the system wavefunction is interrupted by five type of collapses:

$$|\bar{\psi}_c\rangle \rightarrow \hat{C}_\nu |\bar{\psi}_c\rangle \quad |\bar{\psi}_c\rangle \rightarrow \hat{C}_p |\bar{\psi}_c\rangle \quad (5.9)$$

where $\hat{C}_\nu = \sqrt{2}\hat{\nu}$ and $\hat{C}_p = \sqrt{\gamma/\kappa}\hat{\Sigma}_p$ are the collapse operators associated with the five superoperators define in. The collapse probabilities of the wavefunction within a small time interval of length $\Delta(\kappa t)$ are given by

$$p_{c,\nu}(\kappa t) = 2\Delta(\kappa t) \frac{\langle \bar{\psi}_c(\kappa t) | \hat{\nu}^\dagger \hat{\nu} | \bar{\psi}_c(\kappa t) \rangle}{\langle \bar{\psi}_c(\kappa t) | \bar{\psi}_c(\kappa t) \rangle} \quad (5.10)$$

$$p_{c,p}(\kappa t) = 2\Delta(\kappa t) \frac{\langle \bar{\psi}_c(\kappa t) | \hat{\Sigma}_p^\dagger \hat{\Sigma}_p | \bar{\psi}_c(\kappa t) \rangle}{\langle \bar{\psi}_c(\kappa t) | \bar{\psi}_c(\kappa t) \rangle} \quad (5.11)$$

Now we are ready to apply the Monte-Carlo algorithm summarized earlier on chapter 4 to simulate the two-mode cavity QED system subject to a weak external magnetic field.

For the application of the quantum trajectory method, we use a modified program written in Fortran by M. Kronenwett. So as stated before we apply the monte-carlo recipe presented in chapter 4. For the program, we need to take into account certain computational considerations, that we are not going to cover here. Basically this considerations

are for optimization of the code, we reference the reader to [3] to a detailed discussion.

Second-order photon correlation function

Now we present correlation function for the same set of parameteres as in the master equation, but for a larger driving field strength. This are shown in figure (10). We notice that for the non-driven mode the oscillations are no longer there, that at least qualitative is expected with experiments. In this strong excitation regime, we notice that the driven-mode self correlation function and the two-mode crossing-correlation function tend to one. They presents small fluctuations from unity.

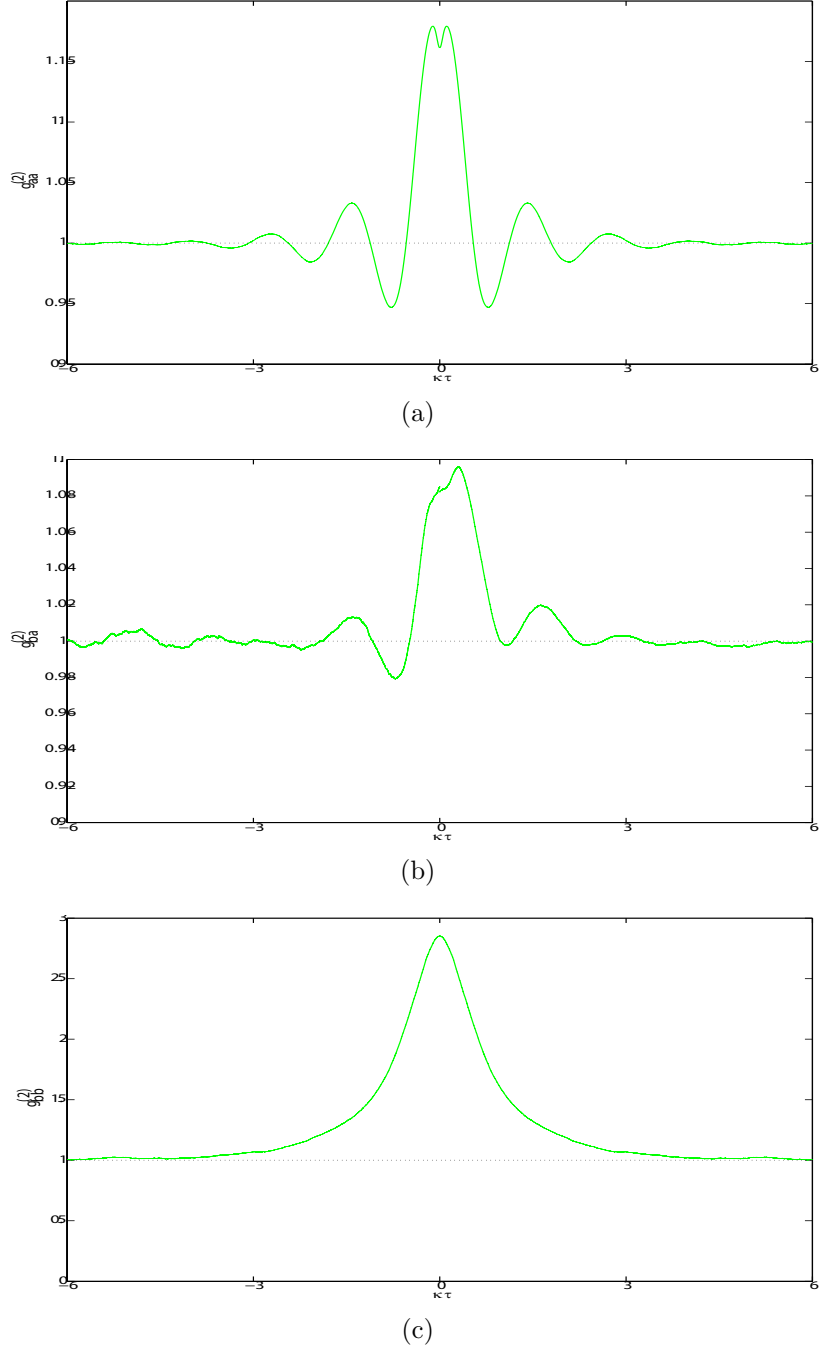


Figure 10: Steady state second-order photon correlation functions for $\gamma/\kappa = 6$, $g/\kappa = 5$, and $\mathcal{E}/\kappa = 6.0$ and $B = 1 \times 10^{-5}\text{T}$: (a) driven-mode self correlation; (b) two mode cross-correlation; (c) non-driven mode self-correlation.

6 Conclusion

6.1 Summary

In this project we have extended the results obtained by Mathias Kronenwet, in order to investigate the dynamics of a cavity QED system where a single atom interacts with two orthogonal linearly polarised cavity modes in the presence of a weak external magnetic field. One cavity mode is driven in resonance by a coherent field, and in the other cavity mode light is being generated only by atomic emission. We calculated the Zeeman effect in the hyperfine structure, and modify the Hamiltonian in order to include the shifting of the energies.

We use quantum regression formulas and a numerical solution of the master equation for a quantitative treatment in the weak-excitation regime, where we made a truncation of the cavity mode Hilbert spaces at two-photon states. From this analysis we observe that the system shows oscillations when subject to a weak external magnetic field. As the driving field becomes stronger the oscillations diminish. This results compare qualitative with the experimental data.

6.2 Future Work

As stated in Kronenwet thesis, there is still future work to be performed. The assumption of an atom at rest in the center of the cavity is not valid. This is due to the fact, that in the experiment single atoms are launched from a magneto-optical trap and experience a varying dipole coupling strength during their flight.

We have assumed that the system is in near resonance, in practice this is only accomplished with limited accuracy. It is important to understand the effect of this detunings in the output.

References

- [1] H.J. Carmichael. *An Open Systems Approach to Quantum Optics*. Springer-Verlag, Berlin Heidelberg, 1993.
- [2] H.C.Wolf H. Haken. *The physics of atoms and quanta: Introducton to experiments and theory*. Springer-Verlag, Berlin Heidelberg, 2004.
- [3] Matthias Kronenwett. *Photon correlations in two-mode cavity quantum electrodynamics*. Master Thesis, The University of Auckland, 2007.
- [4] L. A. Orozco. *From quantum bursts to quantum beats*. http://www.physics.umd.edu/rgroups/amo/orozco/results/2008/CQED_Munich.pdf, 2008.
- [5] M. O. Scully and M. Suhail Zubairi. *Quantum Optics*. Cambridge University Press, United Kingdom, 1997.
- [6] S. M. Tan. *Quantum Optics and Computation ToolBox for MatLab*, 2002.
- [7] M. L. Terraciano, R. Olson Knell, D. L. Freimund, L. A. Orozco, J. P. Clemens, and P. R. Rice. Enhanced spontaneous emission into the mode of a cavity qed sytem. *Optics Letter*, 32:982–984, 2007.